LC Power Passive Filter Circuit for Single Phase Inverter in Residential-Scale Renewable Energy Electricity System Applications

Nurwanti Aprilia Ningrum
Dept. Electrical Engineering
Universitas Hasanuddin
Makassar, Indonesia
ningrumna17d@student.unhas.ac.id

Faizal Arya Samman
Dept. Electrical Engineering
Universitas Hasanuddin
Makassar, Indonesia
faizalas@unhas.ac.id

A Ejah Umraeni Salam
Dept. Electrical Engineering
Universitas Hasanuddin
Makassar, Indonesia
ejah@unhas.ac.id

***Abstract*—This paper illustrates a new method to tune LC filter parameters that will be utilized to attenuate the undesirable harmonic output voltage of DC-AC inverter to generate output waveform approaching pure sinusoidal. This method transforms two-order time-domain equation specification through LC filter transfer function mapping, thus forming simultaneous non-linear equations. This simultaneous equation is solved by applying the Jacobian iteration method until obtaining the required filter parameters. This method offers better results than the existing related methods through Spice simulation in voltage and current THD. The simulation results show the identical voltage and current THD value, which is 0.035%. The parameter values obtained are validated through experiments (hardware testing) to measure THD and the output voltage value with a 5 Watt load, having an impedance of ±50Ω. However, the test results provide a deviation value, specifically for the THD voltage of 11.1% under load conditions and 10.4% under no-load conditions. To date, the causes of the deviation are still analyzed. The deviation is presumably induced by selection of the passive component types that are unsuitable for the power filter application.**

Keywords—Passive power filter, THD, residential scale, single-phase inverter, LC low-pass filter

I. INTRODUCTION

The utilization of renewable energy, notably solar energy, under the recent foremost technology photovoltaic (PV) is the low-carbon energy solution that is widely used globally. For the region with abundant solar irradiation like Indonesia, solar PV is ideal for harnessing solar energy. Solar PV systems allow solar energy to be converted to electricity for centralized or distributed energy resources (DER). Centralized generation by solar farms requires wide-open land with slight shades and above 1 megawatt (MW) capacity. In contrast, DER systems may be ground-mounted or installed on rooftops. DER for residential-scale generally has up to 20 kilowatts (KW) capacity. For commercial, larger public, and industrial building systems, with around 1 MW capacity [1].

Rooftop solar for residential-scale, in particular, is in a much smaller capacity than the other solar PV systems. Nevertheless, this system has many advantages, mainly in democratizing the energy production processes and implementing changes that reduce greenhouse gas emissions. Consequently, it is much more enticing to study rooftop solar for residential-scale. Solar intermittency effects, however, are known as a vexing challenge to the aggregate system. It is caused by varied weather, resulting in uneven solar irradiation, cloud cover, and movement, which generate fluctuating electricity generation and further induce potential instability disturbance to the power system. However, the instability can be regulated through countermeasures [2]. Compared to the utility-scale or large-scale solar farm, rooftop solar feasibly provide minor potential instability disturbance. Due to more viable spatial diversity [3] and bound to be managed by the PV electric control system then supplied to the users first before transmitting the excess power to the utility –primarily applied to the on-grid system. In comparison, sudden loss of supply from solar farms is desired to substantially disturbance the system and challenges system flexibility [4].

Presently, PV systems for both utility grid-connected and stand-alone require a power conditioning unit (PCU) –usually called by solar electric grid controller– a superior technology to convert generated DC power by solar PV to usable AC power. This unit mainly consists of the DC-DC converter, DC/AC inverter, and filter [5]. PCU function to supply required pure sinusoidal voltage wave to maintain the quality of each electronic device provided. For residential-scale, households as the end-user supplied with 220V AC, 50 Hz. Inverter and converter circuit composed by switching a power semiconductor device. The switching produces switching ripple harmonics which affects power quality and brings a problem to the utility [6]. In different circumstances, a filter is the essential part of PCU as the interface between the inverter and the utility due to the ability to attenuate undesirable high harmonic in the system [7].

Therefore, this study proposes analyzing and validating the passive power filter (PPF) circuit of the LC filter. This study further investigated the effects of the PPF circuit and targeted to achieve output according to the IEEE 1547.2-2008 [8] and IEEE 519-2014 [9] standards. The content of the paper is as follows. **Section II** provides related works analysis as a comparative study and to generate hypotheses. The PPF filter is then analyzed theoretically in **Section III** further with the proposed method to tune the filter parameter. **Section IV** and **V** present simulation and experimental results, respectively, as validation processes of the previous method, and **Section VI** concludes the paper.

II. RELATED WORKS ON FILTER ANALYSIS

Ripple harmonics produced by switching the power semiconductor devices are obliged to be attenuated and smoothened. Predicate from early studies, various filter topologies consist of reactive, passive components such as inductor (L) and capacitor (C). It is designed appropriately to be qualified to achieve a standard. However, generating the fault-less filter topology is quite a challenge. The defective design of a passive filter may induce reduced attenuation around the switch-ing frequency, probable resonance among the system impedance, higher price rate of the filters, rise of losses, and possible inductor saturation [7]. Hence, there is a

Under research scheme of "*Riset Inovatif Produktif,* RISPRO Commercial" by LPDP, Ministry of Finance Republic of Indonesia

critical interest in studying a design for filter topology to meet the requirements. As a result, this section presents several publications studies related to LC filter analysis. The LC filter specification design is mentioned in **Table II** to justify the procedure.

A. Design of LC Filter Parameter

For LC filter, a high inductance inductor can smooth the ripple harmonics yet have the aftermath of voltage drop and hold up a response. In comparison, a capacitor connected to the inductor as a shunt establishes low impedance at high frequencies and passes high-frequency harmonics through it. It was suggested to be at low capacitance to hinder high inrush current [6]. Hence, the frequency can block and decrease the number of harmonic frequencies that pass through the system, resulting in reduced current harmonics [10].

Further, a study proposed a design procedure to calculate LC filter component value with four steps. Elaborated algorithm exhibited in the [11]. Value of L_F and C_F is determined with **Eq. (1)** to **Eq. (3)**. **Eq. (1)** obtained the input voltage amplitude at a fundamental frequency that depends on DC voltage and the modulation factor.

$$|V_i(\omega_1)| = m \cdot V_{DC} \tag{1}$$

Where $\omega_1 = 2\pi f_1$. Furthermore, f_1 and m are fundamental frequency and modulation factors, respectively. Then the inductor and capacitor values can be attained from:

$$L_F = \frac{R_{L_m}}{\omega_1} \cdot \sqrt{\alpha^2 - \left(\frac{\omega_1}{\omega_r}\right)^4} \tag{2}$$

$$C_F = \frac{1}{R_{L_m}} \cdot \sqrt{\frac{{\omega_1}^2}{\alpha^2 {\omega_r}^4 - {\omega_1}^4}} \tag{3}$$

Authors in [12] portrayed a three-phase voltage source inverter (VSI) with an LC output filter. The system is described and modeled without employing passive damping and loads, and the point of common coupling (PCC) is directly grounded. Along with the use of inductor and capacitor resistance, each connected series with the respective filter components. The study analyzes filter circuits into a second-order state-space form. Furthermore focuses on proposing an active damping control strategy to damp the filter resonance without fulfilling current feedback. By performing experimental validation with the various scenario of loads, one of the systems with RL load indicated voltage output THD equals 0.845%.

In [13], the authors argued that VSI is referred to as a boost DC-AC converter. Then in the system, the sliding mode controller is proposed. The complex proposed system is explained in the paper. The circuit was quite peculiar due to its system concatenating a current bidirectional boost DC-DC converter, establishing the proposed DC-AC boost converter. A laboratory prototype was implemented and experimented with a voltage output of THD equal to 0.8%.

Other references [14] depicted the design process of LC filter for higher-power class-D amplifiers which above 10 W output power. Although it is a different implication for VSI, the reference is observed and validated, complying with the system described in **Table II**. The equation for the single-phase LC filter utilized indicated as follows:

$$L_F = \frac{R_L \cdot \sqrt{2}}{\omega_1} \tag{4}$$

$$C_F = \frac{1}{\omega_1 \cdot R_L \cdot \sqrt{2}} \tag{5}$$

B. Base Component Analysis

Per unit system representation utilize to normalized quantity or variable of each power system concerning its base value. Since a power system has diverse equipment and each has different voltage power levels later connected, per-unit system avail all the procedures to be quantified and analyzed [15].

TABLE I. BASE VALUES FOR PER UNIT SYSTEM [16]

Parameter	Symbol	Value	Eq.
Rated voltage	V_{RMS}	220V	-
Rated power	S_b	~1300VA	-
Rated angular frequency or Base angular frequency	ω_1/ω_b	$2\pi 50$ Hz	(6)
The base value for voltage defined as peak voltage	V_b	$\sqrt{2/3}V_{RMS}$	(7)
The base value for currents defined as a peak value	I_b	$\frac{S_b}{\sqrt{3}V_{RMS}}$	(8)
The base value for impedance	Z_b	V_b/I_b	(9)
The base value for grid frequency	f_b	50 Hz	-
The base value for filter inductance	L_b	Z_b/ω_b	(10)
The base value for filter capacitance	C_b	$\frac{1}{Z_b \omega_b}$	(11)

In this study, the power filter system utilized the analysis of base values per unit system, which was extensively used to define the value of voltages, currents, powers, and impedance of power equipment [17], definitely the power passive filter parameter. Each value is computed based on **Table I**.

C. Resonant Frequency

The condition where the inductive reactance and the capacitive reactance of the LC filter are equal with the magnitude is defined as the LC filter resonance. The frequency resonant is the frequency which the resonance eventuates. In mathematical terms, the resonance frequency (f_R) is declared as follows: [18]

$$f_R = \frac{1}{2\pi\sqrt{L_F C_F}} \tag{12}$$

D. Cut-off Frequency

To be performed as an appropriate low-pass filter, the system cut-off frequency (f_C) should be determined. A low-pass filter is characterized as passing signals with a frequency lower than the selected f_C and attenuating signals with a frequency higher than f_C. In the mathematical forms, f_C expressed identical with f_R showed in **Eq. (12)**.

E. Series Resistor Damper

Resonance is an inevitable issue that occurs to the high order filters, at which it is required to suppress the resonance [6]. By applying a damping resistor, this resonance frequency can be appropriately damped. Decreasing the quality factor is a decent trade-off between resonance frequency damping, quality factor, filter attenuation, and resistive losses. Passive damping is often implied due to its simplicity and low cost. Where the series damping resistor is calculated on one-third of base impedance (Z_b) [7].

Under research scheme of "*Riset Inovatif Produktif,* RISPRO Commercial" by LPDP, Ministry of Finance Republic of Indonesia

III. Proposed Filter Parameter Tuning Method

This study proposes step-by-step tuning parameters of the filter components, using different approaches from the related works. Information derived from passive filter extracted through transfer function form. Accordingly, the information will be analyzed over the Jacobian iteration method. The diagram for stipulating the passive filter component parameter values is illustrated in **Fig. 1**.

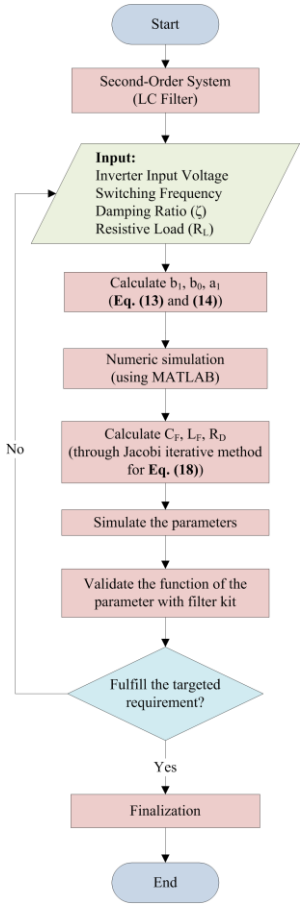

Fig. 1. Flowchart of tuning the parameter of single-tuned LC filter

The PPF used is a single-tuned filter that is the most uncomplicated and inexpensive filtering circuit to attenuate switching ripple harmonics and is solely capable of filtering specific frequency harmonics [19].

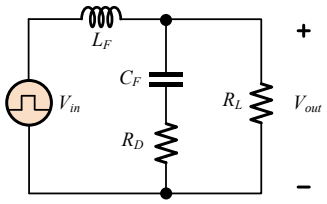

Fig. 2. LC Filter topology

A. Algorithm of Filter Configuration

Passive filter circuits consist of reactive components adept at being evaluated build upon the topologies illustrated in **Fig. 2**, which comprises a capacitor in series with a damping resistor and shunt with the load represented with the resistor. The algorithm is derived from transfer functions of the second-order system, and the analysis of LC filter with transfer function is as follows:

$$H(s) = \frac{V_{OUT}(s)}{V_{IN}(s)} = \frac{b_1 s + b_0}{s^2 + a_1 s + a_0} \quad (13)$$

$$G(s) = \frac{i_{OUT}(s)}{V_{IN}(s)} = \frac{(b_1/R_L)s + 1}{s^2 + a_1 s + a_0} \quad (14)$$

Where

$$b_1 = \frac{C_F R_D R_L}{C_F L_F (R_D + R_L)} \quad (15)$$

$$b_0 = a_0 = \frac{R_L}{C_F L_F (R_D + R_L)} \quad (16)$$

$$a_1 = \frac{C_F R_D R_L + L_F}{C_F L_F (R_D + R_L)} \quad (17)$$

Eq. (13) and **Eq. (14)** were used to derive essential information as the representation of the LC filter's mathematical function and further analyze the performance of the respected filter in reducing ripple harmonics.

B. Jacobian Iteration Method

Under system requirements mentioned in **Section IV**, **Eq. (13)** and **Eq. (14)** as non-linear equations could be solved with an iterative Jacobian method based on **Eq. (18)** where the iterative algorithm may measure the solution of a diagonal linear system if the iterated process converged [20].

$$x(n) = x(n-1) - \left[J\big(x(n-1)\big)\right]^{-1} f\big(x(n-1)\big) \quad (18)$$

LC filter represented its linear time-invariant (LTI) system shown in **Eq. (19)** [21] as the solution for **Eq. (13)**. A low-pass filter such as LC required to be an underdamped system with damping ratio (ζ) measured the rapidity of the oscillations decay from one bounce to the next, in the amount of $\zeta < 1$. The LTI system for LC filter as second-order responses with two poles and one zero is:

$$\frac{V_{OUT}(s)}{V_{IN}(s)} = \frac{b_1 s + {\omega_n}^2}{s^2 + (2\zeta\omega_n)s + {\omega_n}^2} \quad (19)$$

IV. System Description

The power passive filter used for the residential-scale single-phase inverter converts the DC voltage from a solar panel. **Fig. 3** indicates the schematic diagram of the inverter circuit, which its output voltage enacts as the input voltage of the filter circuit.

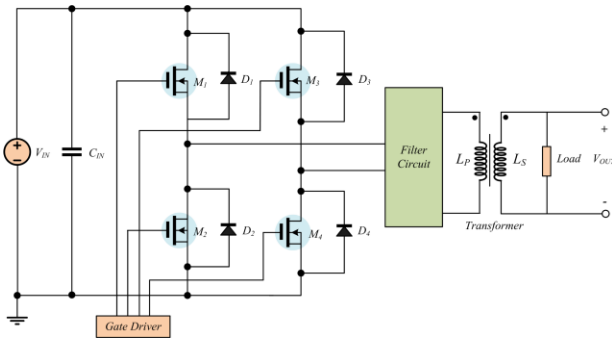

Fig. 3. Inverter Circuit as Input Voltage of Filter Circuit

The filter specifications are illustrated in **Table II**. At the same time, the requirement needed to meet according to IEEE-519 2014 depicted in **Table III** and **Table IV** for the voltage and current distortion limits, respectively. The resulting tuned filter parameters are portrayed in **Table V**.

Under research scheme of "*Riset Inovatif Produktif,* RISPRO Commercial" by LPDP, Ministry of Finance Republic of Indonesia

TABLE II. FILTER SPECIFICATION

Symbol	Meaning	Value
V_{DC}	DC input voltage	36 V
V_{OUT}	Output phase RMS voltage	~220 V
f_s	Switching frequency	10 kHz
f_N	Natural frequency	50 Hz
f_g	Grid fundamental frequency	50 Hz
ΔI_{L1}	Inverter current ripple	20%
ζ	Damping ratio	0.07

TABLE III. VOLTAGE DISTORTION LIMITS ACCORDING TO IEEE-519 [9]

Bus Voltage V at PCC	Individual Harmonic (%)	THD (%)
V ≤ 1.0kV	5.0	8.0
1kV < V ≤ 69kV	3.0	5.0
69kV < V ≤ 161kV	1.5	2.5
161.001kV < V	1.0	1.5

TABLE IV. CURRENT DISTORTION LIMITS FOR SYSTEMS RATED 120 V THROUGH 69 KV ACCORDING TO IEEE-519 [9]

Maximum harmonic current distortion in percent of I_L
Individual harmonic order (odd harmonics) in percent (%)

I_{SC}/I_L	$3 \le h < 11$	$11 \le h < 17$	$17 \le h < 23$	$23 \le h < 35$	$35 \le h \le 50$	TDD
< 20*	4.0	2.0	1.5	0.6	0.3	5.0
20 < 50	7.0	3.5	2.5	1.0	0.5	8.0
50 < 100	10.0	4.5	4.0	1.5	0.7	12.0
100 < 1000	12.0	5.5	5.0	2.0	1.0	15.0
> 1000	15.0	7.0	6.0	2.5	1.4	20.0

Even harmonics are limited to 25% of the odd harmonics.
Current distortions that result in a DC offset, e.g., half-wave converters, are not allowed.
*All power generation equipment is limited to these values of current distortion, regardless of actual I_{SC}/I_L where:
I_{SC} = maximum short-circuit current at PCC (Point Common Coupling)
I_g = maximum demand load current (fundamental frequency component) at the PCC under average load operating conditions

TABLE V. TUNED FILTER PARAMETERS

Symbol	LC Filter Parameter					
	[11]	[12]	[13]	[14]	Proposed Method[1]	Proposed Method[2]
L_F [mH]	80	0.175	550	225.079	20	40
C_F [µF]	300	85	80	0.45	499	249.5
R_D [Ω]	6	N/A	N/A	N/A	0.1002	0.2004
R_L [Ω]	50	33	170	50	50	100
f_r [Hz]	32.487	1304.943	23.994	500.088	50.380	50.380

[1,2]Proposed tuning parameter method analysis with different initial R_L

V. SIMULATION RESULTS

Initial data retrieval was executed by simulating the filter parameter with MATLAB and PSpice AD Lite software. It used square wave (SW) and sinusoidal pulse width modulation (SPWM) as the switching control signal for the gate driver input. The time responses simulation accomplished 500ms to exhibit the steady output after its transient. **Table VI** indicates the reference system in a system condition without a filter.

Table VII denoted the output of each LC filter parameter simulated. The result showed that the switching control used will affect its THD. In comparison, the SW generated a high level of harmonic distortion, which violates the IEEE standards. Therefore, in the next step of validating the filter parameter, the switching control merely employed SPWM. The comparison with the simulation result of the system without filter and with a filter using SPWM exhibited significant effects on mitigating harmonic distortion, hence its low rate of THD values both to its voltage and its current.

TABLE VI. SIMULATION RESULTS SYSTEM WITHOUT FILTER

Switching Control	Output Voltage		Output Current		THD (%)	
	RMS	Peak	RMS	Peak	V	I
SW	4.417	4.403	88.069m	88.341m	47.517	47.517
SPWM	21.639	33.757	432.783m	675.135m	60.832	60.832

The simulation results categorize its responses into two parts, such as time responses and frequency responses. From the simulation results in **Fig. 4** to **Fig. 17**, the outputs waveforms are represented with the color of black for the related work analysis parameters and red for the parameters of the proposed method.

A. Time Responses

The voltage and current outputs become the main parameters to be noticed. **Fig. 4** to **Fig. 7** respectively visualized the time responses for voltage and current output of the simulated systems corresponding with **Table VII**.

TABLE VII. SIMULATION RESULTS SYSTEM WITH LC FILTER

Filter Circuit	Switching Control	Output Voltage (V)		Output Current (A)		THD (%)	
		RMS	Peak	RMS	Peak	V	I
[11]	SW	3.183	7.8643	87.632m	90.749m	4.474	47.781
	SPWM	10.736	20.040	214.717m	400.794m	0.867	0.867
[12]	SW	4.716	11.102	87.899m	107.425m	63.44	47.027
	SPWM	37.755	90.810	1.144	2.752	176.63	176.63
[13]	SW	4.215	7.576	25.987m	26.227m	94.457	47.501
	SPWM	5.501	15.745	32.358m	92.615m	0.086	0.086
[14]	SW	26.377	64.579	88.067m	88.734m	1053.5	47.507
	SPWM	10.561	17.589	211.213m	351.786m	2.839	2.839
Proposed Method[1]	SW	60.585	102.549	56.252m	104.625m	0.231	119.81
	SPWM	107.381	161.668	2.148	3.233	0.017	0.017
Proposed Method[2]	SW	81.077	147.425	33.211m	52.488m	0.183	82.746
	SPWM	113.058	170.859	1.131	1.709	0.035	0.035

[1,2]Proposed tuning parameter method analysis with different initial R_L

From **Fig. 4** to **Fig. 7**, it is distinctly visible that the proposed method with two different initial sets of R_L exhibited a better quality of sinusoidal waveforms than the parameters gathered from the related work analysis, corresponding with the THD value shown in **Table VII**. Exclusively to the output current shown in **Fig 7**, the square wave impaired the outputs for all the simulated systems.

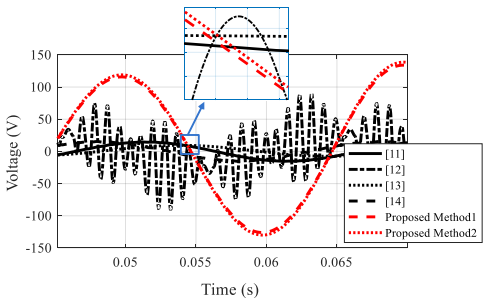

Fig. 4. Output voltage of LC filter circuit with SPWM

B. Frequency Responses

The second-order LC filter topology in **Fig. 1** is analyzed and written as a transfer function shown in **Eq. (13)**. The frequency responses of the simulated systems were then visualized with a bode plot to understand the gain and phase-shift caused by the filter. **Fig. 8** and **Fig. 9** exhibited both the bode amplitude and the bode phase plot.

Under research scheme of "*Riset Inovatif Produktif,* RISPRO Commercial" by LPDP, Ministry of Finance Republic of Indonesia

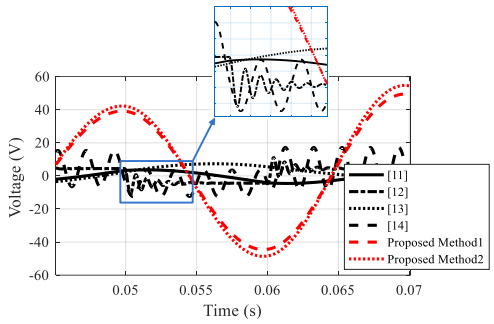

Fig. 5. Output voltage of LC filter circuit with SW

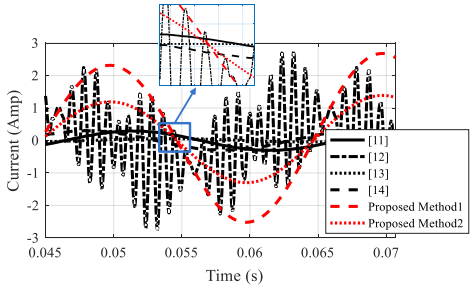

Fig. 6. Output current of LC filter circuit with SPWM

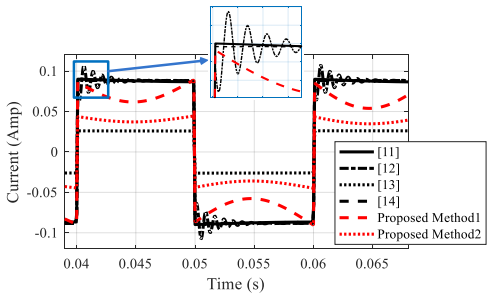

Fig. 7. Output current of LC filter circuit with SW

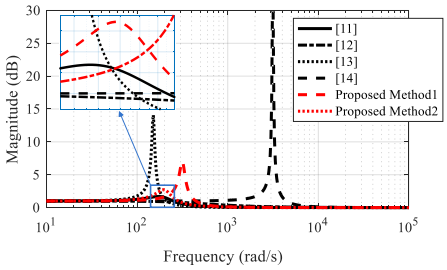

Fig. 8. Bode amplitude plot of LC filter circuit

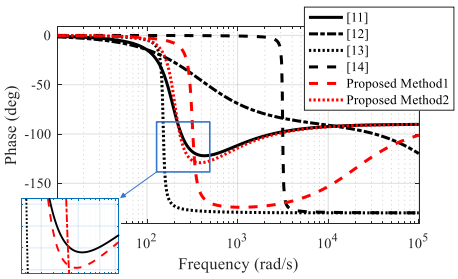

Fig. 9. Bode phase plot of LC filter circuit

Fig. 8 showed six different filter specifications bode amplitude plots. It is inquired that peaking in the magnitude has occurred in each specification, which indicates an f_R. As seen, the related work plot of [14] shed the highest peak, which made the system unstable as a low-filter—followed by peaking value on [13] and proposed method[1]. Later the desired output for the bode magnitude plot appeared in [11], [12], and proposed method[2].

In **Fig. 9**, the bode phase plot indicated the changes in the phase of the sinusoidal signal as it flowed through the system. The phase changes can capture the potential instabilities of the system. In contrast, the attenuation occurred in the six different filter specifications. Parameters from [13] and [14] showed ideal attenuation. Also, both proposed methods revealed attenuation yet still unstable at the higher frequency, then eventually later will be steady on the much further higher frequencies.

C. Harmonic Order

Analysis towards the Fourier component of the output system analyzed with fast Fourier transform (FFT). The result analysis graph portrayed the filter performance attenuating the high frequency. Furthermore, the visualization is divided into two parts, based on its switching control as follows:

a) Using SPWM as Switching Control

Fig. 10 to **Fig. 13** indicated the voltage and current output from the tuned parameters for the related work analysis and proposed method, respectively. Comparing four related work analysis tuned parameters showed that filter performance parameters from [12] are defective due to the emersion of Fourier component in harmonic order around 20 to 50, which corresponds to its THD value shown in **Table VII**, in the amount of 176.63%. Then for the parameters of the proposed method, the set where R_L equals 100 Ω showed better attenuation performance in the higher harmonic order.

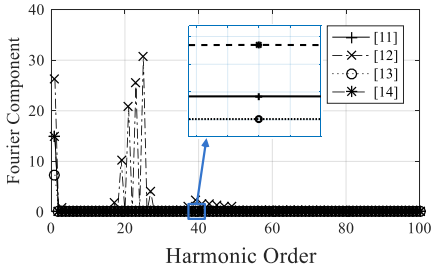

Fig. 10. FFT analysis plot of output voltage of LC filter circuit using SPWM for related work analysis

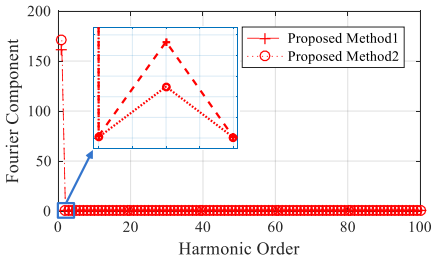

Fig. 11. FFT analysis plot of output voltage of LC filter circuit using SPWM for proposed method

b) Using SW as Switching Control

The voltage and current outputs from the tuned parameters of the [11], [12], [13], [14], and proposed method[1,2], respectively shown in **Fig. 14** to **Fig. 17**. By comparing four related work analysis tuned parameters, it is shown that filter performance parameter from [12] and [14] is defective due to the emersion of Fourier component in harmonic order around 10 to 30, which corresponds to its

Under research scheme of "*Riset Inovatif Produktif,* RISPRO Commercial" by LPDP, Ministry of Finance Republic of Indonesia

THD value shown in **Table VII**, ~60% and ~1000%, respectively. Then, for the proposed method's parameters, the set where R_L equals 100 Ω showed better performance in attenuating the higher harmonic order.

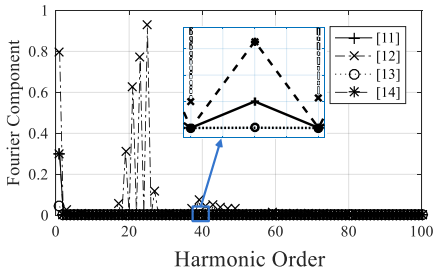

Fig. 12. FFT analysis plot of output current of LC filter circuit using SPWM for related work analysis

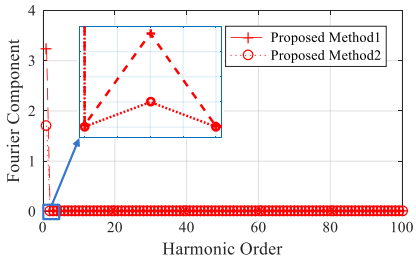

Fig. 13. FFT analysis plot of output current of LC filter circuit using SPWM for proposed method

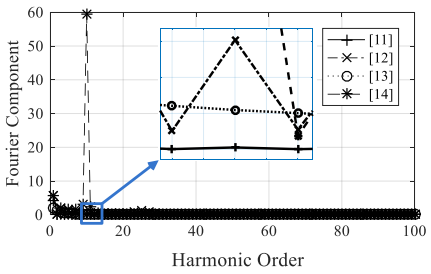

Fig. 14. FFT analysis plot of output voltage of LC filter circuit using SW for related work analysis

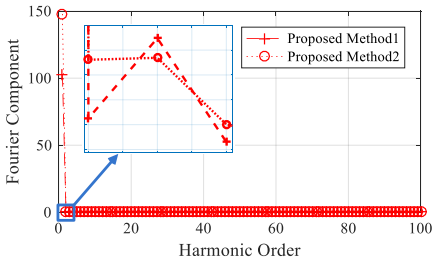

Fig. 15. FFT analysis plot of output voltage of LC filter circuit using SW for proposed method

VI. Experimental Results

A filter kit for experimenting with the filter parameters has been arranged in **Fig. 18** and tested. Tuned filter components values are listed in **Table V**. The filter input originated from AC signal from VSI. The system complied for the filter kit corresponding with **Table II**. The filter output is connected with a 24-220 VAC transformer, and the latter is connected with resistive load, 5 Watt of LED lamp. In comparison, the LED lamp radiance is very bright to all the parameters.

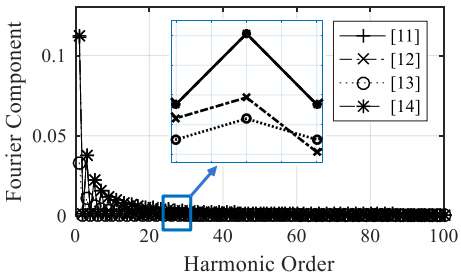

Fig. 16. FFT analysis plot of output current of LC filter circuit using SW for related work analysis

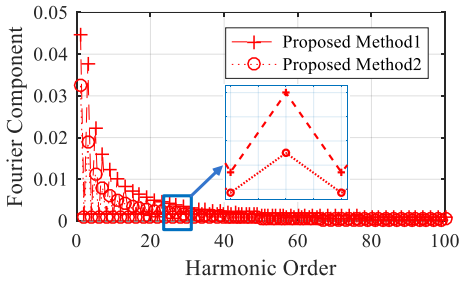

Fig. 17. FFT analysis plot of output current of LC filter circuit using SW for proposed method

Based on the filter parameters in **Table V** and simulation results, the parameters from [12] did not meet the desired standards. **Table VII** portrayed that in comparison with other parameters, parameters from [12] have the highest total amount of THD for both the voltage and the current. Other than that, the output value of voltage and current from [12] showed a significant level of degradation. Hence, exclusively for the parameter from [12], the author did not experiment.

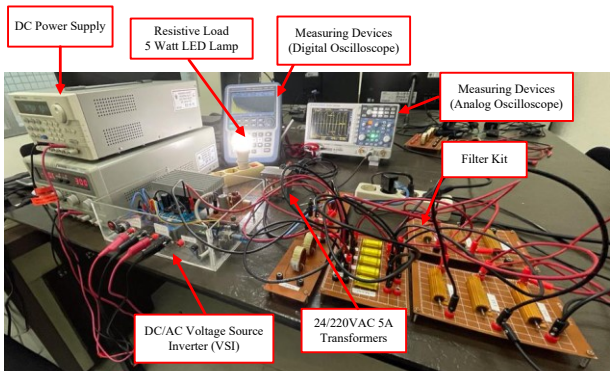

Fig. 18. Experimental Set

In addition, the switching control used in the experimental kit is solely SPWM. Due to the output being corrupted by the SW when complied as switching control. As seen in **Table VII**, SW impaired the THD both to its voltages and currents, and it implied to all tuned parameters. Therefore the output did not meet the desired requirements and was eliminated from the scenario for experimenting. The load condition of the experimental set only used one resistive load. In the experiments, the LED lamp sequentially turns ON then OFF to be compared. **Table VIII** exhibited the experimental results of the system using SPWM.

The measurement of the experimental result using analog and a digital oscilloscope, as shown in **Fig. 18**, visualized the output voltage waveforms and their THD through an FFT

Under research scheme of "*Riset Inovatif Produktif,* RISPRO Commercial" by LPDP, Ministry of Finance Republic of Indonesia

analysis plot. The output displayed is divided based on the tuned filter parameters denoted in **Table V**. Corresponding with **Table VIII**, the output with the nearest result to the desired filter specification shown in **Table II** is the proposed filter[2].

TABLE VIII. EXPERIMENTAL RESULTS SYSTEM WITH SPWM AS SWITCHING CONTROL

Filter Circuit	Load Condition	Output Voltage (V)		THD (%)
		RMS	Peak	V
[11]	OFF	250.0	331.0	14.6
	ON	187.7	240.0	17.1
[13]	OFF	192.7	329.4	23.5
	ON	178.3	277.6	13.6
[14]	OFF	187.6	1.148k	69.6
	ON	168.6	294.9	61.4
Proposed Method[1]	OFF	172.6	243.1	21.8
	ON	140.8	177.3	21.5
Proposed Method[2]	OFF	221.8	316.9	10.4
	ON	213.4	294.9	11.1

A. *Parameters from [11]*

Based on the output graph denoted in **Fig. 19** and **Fig. 20**, these tuned filter parameters indicate tolerable output, albeit not meeting the IEEE standard. It generated a 250VAC of 14.6% voltage THD in an OFF load condition. After the load is switched ON, the voltage rate decreases while the THD increases to 187.7VAC of 17.7% voltage THD.

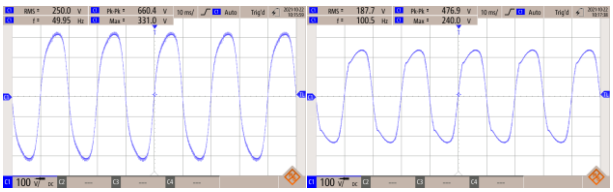

a b

Fig. 19. Voltage output for load condition a) OFF and b) ON

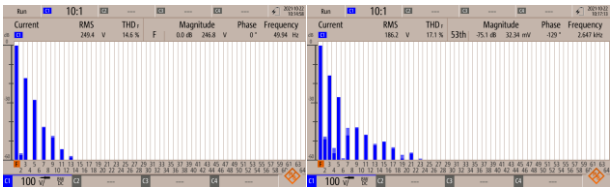

a b

Fig. 20. FFT analysis plot for load condition a) OFF and b) ON

B. *Parameters from [13]*

Fig. 21 and **Fig. 22** displayed an admissible output yet did not meet the standard. It generated a 192.7VAC of 23.5% voltage THD in an OFF load condition. After the load is switched ON, the voltage and THD rate decrease to 178.3 VAC of 13.6% voltage THD.

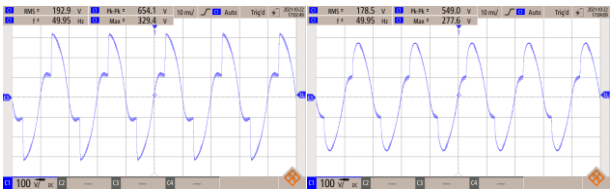

a b

Fig. 21. Voltage output for load condition a) OFF and b) ON

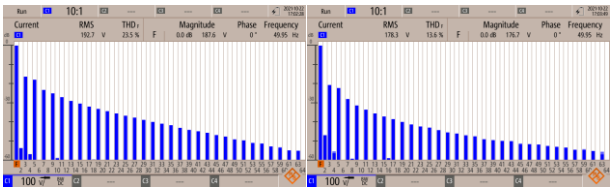

a b

Fig. 22. FFT analysis plot for load condition a) OFF and b) ON

C. *Parameters from [14]*

The output graph denoted in **Fig. 23** and **Fig. 24** of these tuned filter parameters indicated intolerable output and did not meet the IEEE standard. It generated a 187.6VAC of 69.6% voltage THD in an OFF load condition. After the load is switched ON, the voltage rate and the THD value decrease to 168.6VAC of 61.4% THD.

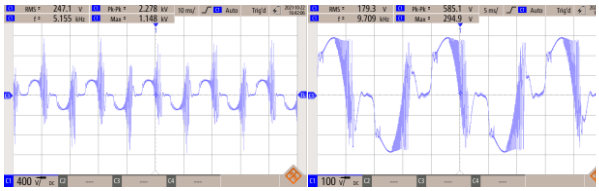

a b

Fig. 23. Voltage output for load condition a) OFF and b) ON

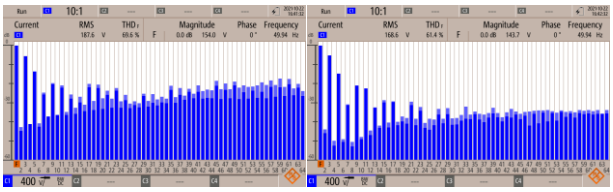

a b

Fig. 24. FFT analysis plot for load condition a) OFF and b) ON

D. *Parameters from Proposed Method[1]*

Fig. 25 and **Fig. 26** exhibited an admissible output yet did not meet the IEEE standard. It generated a 172.6VAC of 21.8% voltage THD in an OFF load condition. After the load is switched ON, the voltage rate and the THD decrease to 140.8VAC of 21.5% voltage THD.

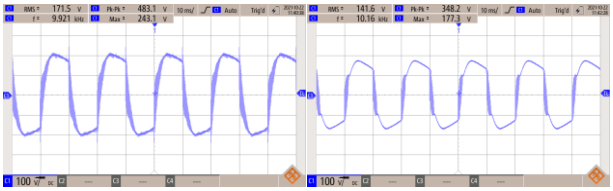

a b

Fig. 25. Voltage output for load condition a) OFF and b) ON

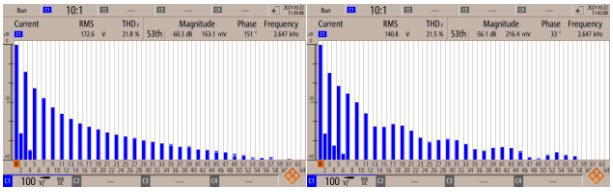

a b

Fig. 26. FFT analysis plot for load condition a) OFF and b) ON

Under research scheme of "*Riset Inovatif Produktif,* RISPRO Commercial" by LPDP, Ministry of Finance Republic of Indonesia

E. *Parameters from Proposed Method*[2]

Fig. 27 and **Fig. 28** denote the output graph of these tuned filter parameters, which both indicate tolerable output and did not meet the IEEE standard. It generated a 221.8VAC of 10.4% voltage THD in an OFF load condition. After the load is switched ON, the voltage rate and the THD value decrease to 213.4VAC of 11.1% voltage THD.

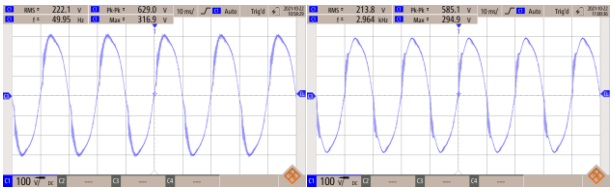

a b

Fig. 27. Voltage output for load condition a) OFF and b) ON

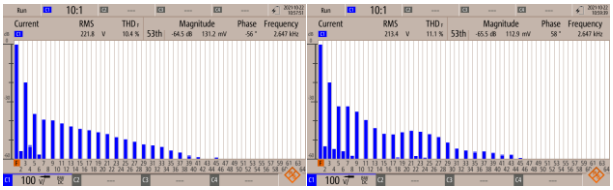

a b

Fig. 28. FFT analysis plot for load condition a) OFF and b) ON

VII. Conclusions

The results of the design using the proposed method provide filter parameter values, among others, L_F of 40mH, C_F of 249.5µF, and R_D of 0.2004 for R_L load of 100Ω. The simulation results using SPWM as an electronic switch control signal and input voltage of 36VDC, giving the same 0.035% voltage and current THD values and 113.058VAC output voltage amplitude. Furthermore, the filter parameters were validated through laboratory-scale experiments with a filter kit. They produced an output voltage of 213.4 VAC, a voltage THD of 11.1% under load conditions, and an output voltage of 221.8VAC, a voltage THD of 10.4% under no-load conditions.

The author recommends where improvements of this paper can be directed to studying the robustness or sensitivity analysis of filter parameters determined by varying the load supplied by the filter output. This method can also be considered to be tested on a filter circuit with an LCL topology. In addition, this study could be developed to be implemented for the high power application filter systems of other DER systems.

Acknowledgment

The authors gratefully acknowledge the Ministry of Finance of the Republic of Indonesia (by *Lembaga Pengelola Dana Pendidikan*-LPDP) for funding our research entitled, 'Innovative Power Electronic Product for Hybrid Renewable Energy based Electric for Future Self-Power Homes' under the scheme of "*Riset Inovatif Produktif,* RISPRO Commercial" starting from August 2019.

Bibliography

[1] Asian Development Bank, Handbook for Rooftop Solar Development in Asia, Mandaluyong City, Philippines: ADB, 2014.

[2] D. Rowe, S. Sayeef and G. Platt, "Intermittency: It is the Short-Term That Matters," in *Future of Utilities - Utilities of the Future*, CA, USA, Academic Press, 2016, pp. 129-149.

[3] J. K. Ward, T. Moore, and S. Lindsay, "The Virtual Power Station - achieving dispatchable generation from small scale solar," in *50th Annual Conference, Australian Solar Energy Society (Australian Solar Council)*, Melbourne, 2012.

[4] S. Impram, S. V. Nese and B. Oral, "Challenges of renewable energy penetration on power system flexibility: A survey," *Energy Strategy Reviews,* vol. 31, pp. 1-12, 2020.

[5] M. K. Mahapatra and P. Singh, "Fuel Cells: Energy Conversion Technology," in *Future Energy (Second Edition): Improved, Sustainable and Clean Options for our Planet*, Connecticut, USA, Elsevier Science, 2014, pp. 517-519.

[6] M. Büyük, A. Tan, M. Tümay and K. Bayındır, "Topologies, generalized designs, passive and active damping methods of switching ripple filters for voltage source inverter: A comprehensive review," *Renewable and Sustainable Energy Reviews,* vol. 62, pp. 46 - 69, 2016.

[7] R. Beres, X. Wang, F. Blaabjerg, C. L. Bak and M. Liserre, "A Review of Passive Filters for Grid-Connected Voltage Source Converters," *IEEE Journal of Emerging and Selected Topics in Power Electronics,* vol. 4, no. 1, pp. 54 - 69, 2015.

[8] IEEE Standards Coordinating Committee 21 on Fuel Cells, Photovoltaics, Dispersed Generation, and Energy Storage, IEEE Application Guide for IEEE Std 1547™, IEEE Standard for Interconnecting Distributed Resources with Electric Power Systems, New York, USA: The Institute of Electrical and Electronics Engineers, Inc., 2008.

[9] IEEE Industry Applications Society/ IEEE Power Engineering Society, IEEE Std 519-2014: Recommended Practice and Requirements for Harmonic Control in Electrical Power Systems, New York, USA: The Institute of Electrical and Electronics Engineers, Inc, 2014.

[10] N. Mahamad, C. M. Hadzer, and S. Masri, "Application of LC Filter in Harmonics Reduction," in *National Power & Energy Conference (PECon)*, Kuala Lumpur, 2004.

[11] A. A. Ahmad, A. Abrishamifar and M. Farzi, "A New Design Procedure for Output LC Filter of Single Phase Inverters," in *2010 3rd International Conference on Power Electronics and Intelligent Transportation System*, Hong Kong, China, 2010.

[12] I. D. de Souza, P. M. de Almeida, P. G. Barbosa, and C. A. Duque, "Digital single voltage loop control of a VSI with LC output filter," *Sustainable Energy, Grids and Networks,* vol. 15, p. 145–155, 2018.

[13] R. O. Caceres and I. Barbi, "A Boost DC–AC Converter: Analysis, Design, and Experimentation," *IEEE Transactions on Power Electronics,* vol. 14, no. 1, pp. 134-141, 1999.

[14] Texas Instruments, "Application Report: LC Filter Design," Texas Instruments Incorporated, Texas, 2016.

[15] National Programme on Technology Enhanced Learning, "Chapter 1: Modelling Power System Components," [Online]. Available: https://nptel.ac.in/. [Accessed 14 09 2021].

[16] F. Thams, J. A. Suul, S. D'Arco, M. Molinas and F. W. Fuchs, "Stability of DC voltage droop controllers in VSC HVDC systems," in *IEEE Eindhoven PowerTech*, Eindhoven, Netherlands, 2015.

Under research scheme of "*Riset Inovatif Produktif,* RISPRO Commercial" by LPDP, Ministry of Finance Republic of Indonesia

[17] The MathWorks, Inc., "Per-Unit System of Units," MathWorks, 2021. [Online]. Available: https://www.mathworks.com. [Accessed 30 July 2021].

[18] M. Gong, Z. Tan, X. Yuan, and X. Wu, "System and Method for Damping LC Circuits in Power Conversion Systems." United States of America Patent 8,295,063 B2, 23 October 2012.

[19] C. Bo, Z. Xiangjun and X. Yao, "Three Tuned Passive Filter to Improve Power Quality," in *International Conference on Power System Technology*, Chongqing, China, 2006.

[20] S. Yousef, "Chapter 13: Multigrid Methods," in *Iterative Methods for Sparse Linear Systems Second Edition*, Philadelphia, Society for Industrial and Applied Mathematics, 2003, pp. 414-416.

[21] M. T. Thompson, "Review of Signal Processing Basics," in *Intuitive Analog Circuit Design*, Amsterdam, Elsevier, 2014, pp. 15-52.

Under research scheme of "*Riset Inovatif Produktif,* RISPRO Commercial" by LPDP, Ministry of Finance Republic of Indonesia